April 2011

Swimming of Undulating Filaments in Viscous Fluids

Tristan David Spoor
Worcester Polytechnic Institute

Swimming of Undulating Filaments in Viscous Fluids

A Major Qualifying Project Report

submitted to the Faculty

of the

WORCESTER POLYTECHNIC INSTITUTE

in partial fulfillment of the requirements for the

Degree of Bachelor of Science

by

Tristan Spoor

Advisors: Stephan Koehler, B.S. Tilley

April 28, 2011

Abstract

Swimming of microorganisms in viscous fluids is a complex problem involving many degrees of freedom. In order to gain insight to this problem we investigate resistive force theory as a model for thin undulating filaments at low Reynolds number. The filaments are sufficiently thin so that resistive force theory can be used. We compare four major waveforms, which have one adjustable parameter; they are the square wave, sawtooth, cartesian sine, and curvature sine. The main quantities of interest are the swimming speed and swimming efficiency. For the infinitely long filaments motion is unidirectional along the center-line and the sawtooth is found to be the fastest and most efficient method. The swimming behavior of short filaments is far more complex, because there is cyclic pitching, and the velocity is periodic. Arguments about the symmetry are presented and it is noted that there is an optimal pitching state around half-integer wavelengths. We perform numerical parametric studies in terms of the filament length and actuation parameter and again find the sawtooth strategy to be the fastest and most efficient. We also provide Taylor-series solutions for the swimming of short filaments.

Contents

1 Background

Locomotion of micro-organisms is a complex problem that has been studied by many different fields [1, 2, 3]. Biologists study swimming at a molecular and cellular level, looking to real life specimens for their studies [4, 5, 6]. At the same time, engineers are concerned with the direct mechanics and how they can emulate them. The focus of this study is in the fundamental principles behind swimming in fluids where viscous effects are dominant.

Micro-organisms swim in viscous fluids where inertial effects are negligible. This low Reynolds number swimming has been the focus of many studies and the first investigation into this field is by G. I. Taylor [7]. Taylor calculated the swimming speed and efficiency of a sinusoidally undulating infinite sheet. He finds that the direction of propagation was opposite to the direction of motion, however the solutions he finds are valid for small amplitude undulations. Taylor's research spurred later work by Gray and Hancock who were able to extend the ideas to infinite length undulating filaments [8].

The hydrodynamics of swimming are very complicated and as a result Gray and Hancock developed resistive force theory to create a model with which they could find an optimal speed and efficiency for a swimming filament[8]. Resistive force theory is a simplified model that is based on the assumptions that hydrodynamic effects are negligible on a sufficiently thin filament, and that the force distribution along a filament depends on the local velocity. Resistive force theory is discussed in more detail later on. Using this model they were able to investigate sawtooth and sinusoidal swimming strategies [8].

This led to a number of focused studies into simplified swimming. Resistive Force Theory

was further modified by Keller and Rubinow [9] and J. Lighthill [10] to apply to filaments of finite thickness. Additionally Lighthill investigated the sawtooth strategy and found that the most efficient strategy was one with a slope angle of $\approx 40°$. Later studies considered the minimal "Purcell Swimmer" that consists of three links with rotating joints[11, 12, 13]. This swimmer was studied using resistive force theory and an optimal swimming strategy for speed was found.

The most recent studies have focused on finite length swimmers and have begun to consider the physiological constraints imposed on the swimming problem. Pironneau and Katz [14] study sinusoidal strategies where the filament length was an integer of the wavelength. They note that efficiency increases with the number of wavelengths attached, and attributed it to a decrease in pitching. Spagnolie and Lauga [15] studied finite length sawtooth strategy swimmers. They considered elastic effects and found that the efficiency had local maxima for filament lengths that that were half-integer multiples of the wavelength.

This study uses resistive force theory to find maximal efficiencies and swimming speeds for four different waveforms: sawtooth, square, cartesian sine, and curvature sine. Symmetries of the filament are examined which shed insight into the aforementioned local efficiency maxima for filament lengths which are a slightly less than half-integer multiples of the wavelength. Additionally three different length scales are investigated: infinite, intermediate, and small amplitude.

As noted earlier the full hydrodynamic problem is very difficult to solve and as a result we choose to introduce some constraints. The first is that our filament will be confined to the

$x - y$ plane. We require that our filament is inextensible. We also assume that the filament is thin enough such that hydrodynamic effects are negligible and resistive force theory is applicable.

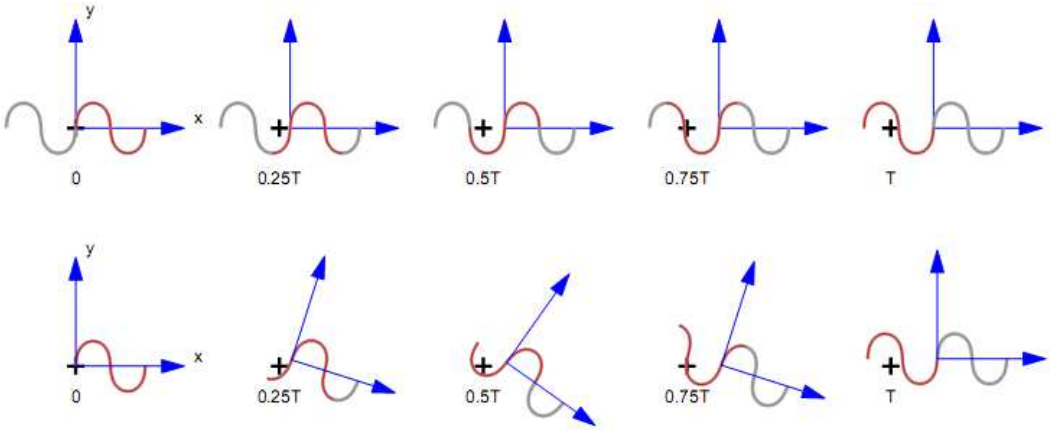

Figure 1: Cartoon sequence of the swimming motion for the curvature sine strategy, $\alpha = 1.5$, at times $t/T = 0,\ 1/4,\ 1/2,\ 3/4,\ 1$. The top row is for an infinitely long filament, and the gray background curve shows the waveform through which the filament is "pulled'. The bottom row is for $S = 0.5\lambda$, and the gray background curve shows the tracks left by the swimmer in the Lagrangian frame. The Eulerian origin is denoted by a heavy "+", and the Lagrangian frame by the arrows, which moves to the right and rotates. This rotation during translation is called pitching.

The top row of cartoons of Fig. 1 illustrate the swimming process for the curvature sine waveform for an infinite filament, which may be viewed as a video in Appendix A. Denote the filament length S and the arc length s. We observe the filament in two different frames. In the Lagrangian frame $\mathbf{r}_{\mathrm{L}}(s,\ t)$ we dictate a waveform along which the filament deforms.

The waveform is defined by a periodic waveform of arc length q, $\mathbf{r}_{\mathrm{L}}(q)$. The filament travels through the shape $\mathbf{r}_{\mathrm{L}}(q-vt)$, with wave speed v. At any give time the filament extends from $q = vt$ to $q = S + vt$, and deforms as it travels down the wave. By dictating the waveform we know that the velocity in the Lagrangian frame is proportional to the tangent vector, $\mathbf{u}_{\mathrm{L}} = v\hat{\mathbf{t}}$.

Simultaneously in the Eulerian frame, $\mathbf{R}(s,\ t)$, we observe the position of the swimming filament and calculate the total velocity. The filaments position in the Eulerian frame is given by

$$\mathbf{R}(s,\ t) = \mathbf{R}_L(t) + \mathcal{R}_{\Theta_L(t)}\mathbf{r}(s,\ t) \tag{1}$$

where $\mathbf{R}_L(t)$ is the location of the Lagrangian's origin, and $\Theta_L(t)$ is the pitching angle. The total velocity is a combination of the velocity of Lagrangian frame and the velocity due to the swimming mechanics of the filament,

$$\dot{\mathbf{R}}(s,\ t) = \dot{\mathbf{R}}_L(t) + \mathcal{R}_{\Theta_L(t)}\left(\dot{\theta}(t)\hat{\mathbf{n}}(s,\ t) + v_0\hat{\mathbf{t}}(s,\ t)\right)\ , \tag{2}$$

With the following setup in place we are ready to consider the dynamics of these filaments. We calculate two quantities of interest, the swimming speed and the swimming efficiency using resistive force theory. We set up the force and torque integrals accordingly,

$$\mathbf{F} = \xi\int_{s=0}^{S} 2(\dot{\mathbf{R}}(s,\ t)\cdot\hat{\mathbf{n}})\hat{\mathbf{n}} + (\dot{\mathbf{R}}(s,\ t)\cdot\hat{\mathbf{t}})\hat{\mathbf{t}}ds \tag{3}$$

$$\boldsymbol{\tau}(t) = \xi\int_{s=0}^{S} \mathbf{R}(s,\ t)\times d\mathbf{F}(s,\ t)ds \tag{4}$$

We know that a filament in a fluid must satisfy a force and torque free condition, which allows us to set these integrals equal to zero. This gives a set of three equations, force balance in x and y as well as a torque balance that solves for $\Theta_{\mathrm{L}}(t)$ and $\mathbf{R}_{\mathrm{L}}(t)$. These solutions can then be substituted into the equation for $\mathbf{r}(s,\ t)$, and form a set of three ODE's that can are then solved to produce the position and swimming velocity.

2 Performance Criteria

In order to compare our swimmers a number of performance criteria are discussed. The first two criteria have been classically used to address the swimming problem[7, 1]. The first is a comparison of the speed of the swimmer to the wave speed

$$\tilde{U}_{v_0} = U/v_0 = D/\lambda \tag{5}$$

The second is a comparison of the work required to move a straightened filament the same distance in the same amount of time as the work required to undulate that filament $\mathcal{W}$

$$\tilde{\mathcal{W}}_{v_0} = \xi UDS/\mathcal{W} \tag{6}$$

In this criteria ξUDS is the work for pulling a straight filament. These classical criteria were originally developed around infinite waveforms for which the only available length scale is λ. When we began applying the performance criteria to finite length swimmers we noted another possible length scale the length of the filament S. However when we used this new performance criteria of D§ the results were counter intuitive. Upon further investigation it

was found that one could redefine the wavelength of a given strategy as 2λ, which resulted in double the displacement for the redefined undulation and therefore artificially doubles the efficiency.

To solve this problem two new performance criteria are presented which share a few fundamental ideas. Both strategies compare the performance of the swimming filament to that of a straight dragged filament. They also both rely on the assumption that optimal efficiency swimming occurs when there is uniform power expenditure. This is intuitively seen by noting that if someone is creating a machine with optimal efficiency part of that design will have it run at constant power. You can also see this in the infinite case which has the highest efficiency of any swimmer and does so at constant power. In order to define these new criteria the time required to undulate the filament one period at constant power is introduced

$$T_{\mathcal{P}_0} = \frac{1}{v_0} \int_0^{\lambda} \sqrt{\frac{\mathcal{P}(v_0, s/v_0)}{\mathcal{P}_0}} ds \tag{7}$$

Where $\mathcal{P}_0 = \xi \left(D/\left(\lambda/v_0\right)\right)^2 S$ is the power required to pull a straightened filament. Using this time we formulate the speed ratio of a dragged to undulated filament at constant power

$$\tilde{U}_{\mathcal{P}_0} = \frac{\lambda/v_0}{T_{\mathcal{P}_0}} \tag{8}$$

And lastly comparing the work expended by one undulation of the swimming filament with that expended by dragging the straight filament the same distance in the same amount of

time both at constant power

$$\tilde{\mathcal{W}}_{\mathcal{P}_0} = \frac{\xi\left(\frac{D^2}{T_{\mathcal{P}_0}}\right) S}{\mathcal{P}_0 T_{\mathcal{P}_0}} = \left(\frac{\lambda}{v_0 T_{\mathcal{P}_0}}\right)^2 \tag{9}$$

This however is just the square of $\tilde{\mathcal{W}}_{v_0}$ and so will be neglected in favor of $\tilde{\mathcal{W}}_{v_0}$.

3 Waveforms

This section describes each of the four waveforms, Sawtooth, Square, cartesian Sine, and Curvature sine, in terms of parameterization and construction. These are the waveforms along which the filament is actuated.

3.1 Sawtooth and Square Wave

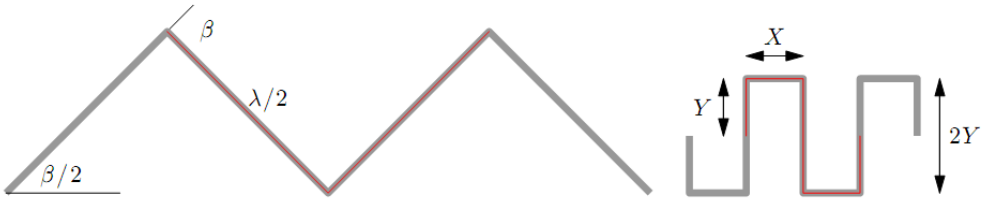

Figure 2: Sawtooth and square. Here the slope angle of the sawtooth is $\alpha = \pi/4$, and $X = Y/2 = \lambda/6$. The light gray curve in the background shows the continuation of the waveform.

The first two waveforms, square and sawtooth, are discontinuous, but fairly easy to parameterize. As shown in Fig. 2 the sawtooth is parameterized in terms of the bending

angle β between successive links. The bending angle has a range of $0 \leq \beta \leq \pi$. The square is a sawtooth wave with $\beta = \pm\pi/2$ that has two positive bends followed by two negative bends. Here the duty cycle is parameterized in terms of the width of the horizontal segment X. The possible ranges for this width are $0 \leq X \leq \lambda/2$.

3.2 Sinusoidal Waves

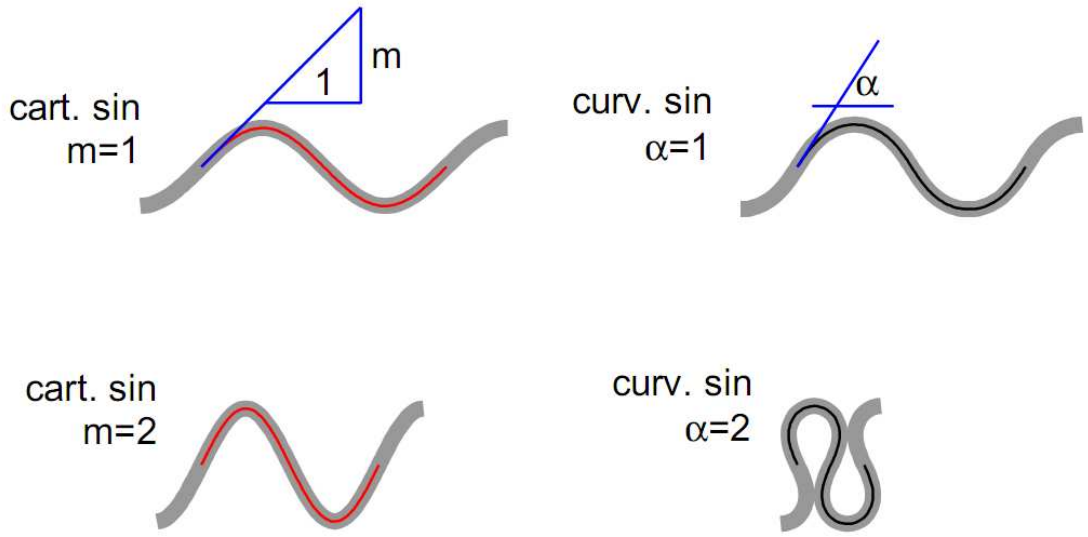

Figure 3: Swimming sinusoids with total length equaling one wavelength. The cartesian sine waves are parameterized by $y = \frac{m\lambda}{2\pi} \sin\left(\frac{2\pi x}{\lambda}\right)$, whereas the curvature sine waves are parameterized in terms of their local curvature $\kappa = \frac{2\pi\alpha}{\lambda} \sin\left(\frac{2\pi s}{\lambda}\right)$. The light gray curve in the background shows the continuation of the waveform.

The sinusoidal shapes are slightly more complex in their construction. The cartesian

sine dictates the actuation of the filament through its waveform, however the curvature sine dictates the actuation through curvature. As shown in Fig. 3 the cartesian sine is the sinusoidal function $y = a\sin(x)$, and the related curvature sine is given by a sinusoidally varying curvature $\kappa = \frac{2\pi\alpha}{\lambda}\sin\left(\frac{2\pi s}{\lambda}\right)$. For small amplitude undulations the curvature and cartesian sine are the same because of the small angle approximation. In order to construct the curvature sine we start by expressing its tangent in terms of θ the angle the tangent makes with the x-axis:

$$\hat{\mathbf{t}} = \begin{bmatrix} \cos(\theta) \\ \\ \sin(\theta) \end{bmatrix} . \tag{10}$$

which when solved for the curvature yields:

$$\theta = \alpha\cos\left(\frac{2\pi s}{\lambda}\right) . \tag{11}$$

The curvature sine is parameterized by α which is the initial slope angle (at $s = 0$). For values of $\alpha > \pi/2$ the curvature sine becomes multivalued, and for sufficiently high values of α the function becomes self intersecting. The cartesian sine is defined as

$$y = \frac{m\lambda}{2\pi}\sin\left(\frac{2\pi x}{\lambda}\right) \tag{12}$$

and is parameterized in terms of the value of its slope at the origin, m.

4 Infinite Swimmers

In this section we present analytic solutions for arbitrary amplitude infinite swimming filaments. We consider the same four waveforms that are presented in the finite and numerical

cases: sawtooth, square, curvature sine, and cartesian sine. We use the axioms of resistive force theory, as well as several simplifications unique to the infinite case, to compute exact analytical answers where possible or a Taylor approximation where necessary. We compute the average speed of the filament as well as its efficiency.

Previous work in this area has considered either only the sawtooth waveform, or restricted its analysis to small amplitude. Work by G. I. Taylor [7] and Gray and Hancock [8]addressed small amplitude infinite cartesian sine swimmers. We reproduce their results and expand them to larger amplitude. Work by J. Lighthill addressed an infinite arbitrary amplitude sawtooth swimmer. Lighthill determined the optimum efficiency occurs when the bending angle is $\beta = 84°$ [1], which our results closely support. We present new expressions for the infinite square wave and the infinite curvature sine.

The infinite analysis is used to compare to and verify the numerical simulations that appear later in this report. The numerics were run in Matlab using a quadrature rule to evaluate the force and torque balances 4, and then `ode45` was used to solve the differential equation 2 for $\dot{\theta}$ and $\dot{\mathbf{R}}_L(t)$. The infinite strategies are analyzed to determine the optimal swimming parameters and are compared with each other.

4.1 Simplifications

There are three simplifying assumptions that can be made for an infinite filament. The first two assumptions come from the symmetry of the infinite filament. First we can state that there is no force in the y-direction. This comes from the fact that every force in the y-

direction will be balanced by an equal but opposite force elsewhere on the filament. Similarly we can state there will be no rotation as the torques along the filament are balanced. The last assumption is that there is no time dependence. This follows from an infinite filament having the same shape at all times.

The equation for local velocity becomes

$$\mathbf{U}_{\mathrm{E}} = U_x\hat{\mathbf{x}} + v_0\hat{\mathbf{t}} \ , \tag{13}$$

where $U_x\hat{\mathbf{x}}$ is the velocity of the Lagrangian frame. Moreover, for the infinite case the force and torque balance equations simplify down to balancing the force along the x-direction. Another simplification for the infinite case is that the power dissipated per wavelength is constant, and therefore only two efficiency criteria need to be evaluated: $\tilde{U}_{v_0}$ and $\tilde{\mathcal{W}}_{v_0}$.

4.2 Sawtooth

A filament traveling along the sawtooth wave has two different vectors, depending on the location. In the Lagrangian frame these are:

$$\hat{\mathbf{t}}_1 = \begin{pmatrix} \cos(\beta/2) \\ \\ \sin(\beta/2) \end{pmatrix}, \hat{\mathbf{t}}_2 = \begin{pmatrix} \cos(\beta/2) \\ \\ -\sin(\beta/2) \end{pmatrix} \tag{14}$$

From the infinite simplifications the sawtooth is moving only in the x-direction. Accordingly, using the expression for local velocity, $U_x\hat{\mathbf{x}} + v_0\hat{\mathbf{t}}$, and Eq. 4 the force is:

$$\mathbf{F}_x = \xi\lambda\left(2U_x + \cos(\beta/2)v_0 - \cos(\beta/2)^2U_x\right) \tag{15}$$

Setting $F_x = 0$ for the force balance gives $U_x = -\cos(\beta/2)/(2+\cos(\beta/2)^2)$. The net velocity is obtained by integrating $U_x + v_0 t_x$ over one undulatory cycle

$$D_x = \mathrm{sgn}(v_0)\lambda \frac{\cos(\beta/2)(1-\cos(\beta))}{3-\cos(\beta)} \tag{16}$$

The power expended by one wavelength is calculated as

$$\begin{aligned} P &= \int_0^\lambda [2(-U_x \sin(\beta/2) + 2\cos(\beta/2)\sin(\beta/2))^2 \\ &+ (U_x \cos(\beta/2) - \cos(\beta/2)^2 + \sin(\beta/2)^2)^2] ds \\ &= \xi v_0^2 \lambda \frac{2\sin(\beta/2)^2}{2-\cos(\beta/2)^2} \end{aligned} \tag{17}$$

And finally compare the calculated power with the power required to move a straight filament to get the efficiency.

$$\tilde{\mathcal{W}}_{v_0} = \frac{\sin(\beta/2)^4(1-\sin(\beta/2)^2)}{2(\sin(\beta/2)^2+1)(1-(\sin(\beta/2)^2+1))} \tag{18}$$

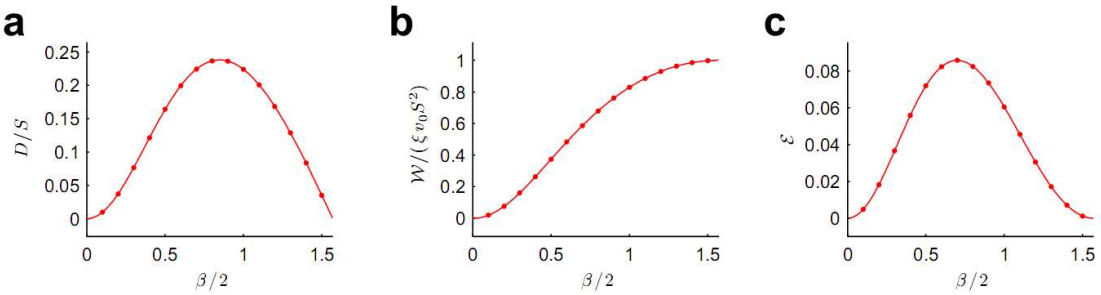

Figure 4: Comparison of the analytical to numerical results for the infinite sawtooth.

Fig. 4 shows close agreement between the analytic solutions and the numerical results for long filaments for all values of β. The optimum for the normalized speed occurs at $\beta = 1.694$, $\tilde{U}_{v_0} = .2376$. The optimum for the normalized work from occurs at $\beta = 1.398$, $\tilde{\mathcal{W}}_{v_0} = .0858$.

The optimal angle is 80.12 which agrees closely with Katz and Pironeaus value of 80 for the finite filament [14], and is in reasonable agreement with Lighthill's result of 84° [1].

4.3 Square

A filament traveling along the square wave has three different vectors. In the Lagrangian frame these are $\hat{\mathbf{t}}_1 = \hat{\mathbf{y}}$, $\hat{\mathbf{t}}_2 = \hat{\mathbf{x}}$ and $\hat{\mathbf{t}}_3 = -\hat{\mathbf{y}}$. The local velocity of points on the filament are $U_x + v_0 t_x$, and from Eq. (4) the total force is given by summing the contributions due to the vertical and horizontal segments of the square wave.

$$\mathbf{F}_x = \xi(\mathbf{F}_{\text{horiz}} + \mathbf{F}_{\text{vert}}) = \xi([2X(U_x + 3v_0)] + [2Y(2U_x)]) \tag{19}$$

where $Y = \lambda/2 - X$. Setting $F_x = 0$ for the force balance gives $U_x = (-v_0 X)/(\lambda - X)$. The net velocity is obtained by integrating $U_x + v_0 t_x$ over one undulatory cycle

$$D_x = \text{sgn}(v_0)\lambda \frac{X\,(\lambda - 2X)}{\lambda(\lambda - X)}\,. \tag{20}$$

Where $\text{sgn}(v_0)$ denotes the sign of v_0. The power expended by one wavelength is the sum of the power on the four different segments

$$\mathcal{P} = 2\mathbf{F}_{\text{horiz}} \cdot (U_x + v_0\hat{\mathbf{x}}) + 2\mathbf{F}_{\text{vert}} \cdot (v_0\hat{\mathbf{y}}) = \xi v_0^2 \left[\frac{4X^2(2\lambda^2 - 5\lambda X + 2X^2)}{\lambda^2(\lambda - X)}\right]. \tag{21}$$

Finally the work efficiency is the calculated power compared with the power required to move a straight filament.

$$\tilde{\mathcal{W}}_{v_0} = \frac{X^2(2X - \lambda)}{\lambda(X^2 - \lambda^2)} \tag{22}$$

Fig. 5 again shows close agreement between the analytic solutions and the numerical results for long filaments for all values of X. The optimum for the normalized speed occurs

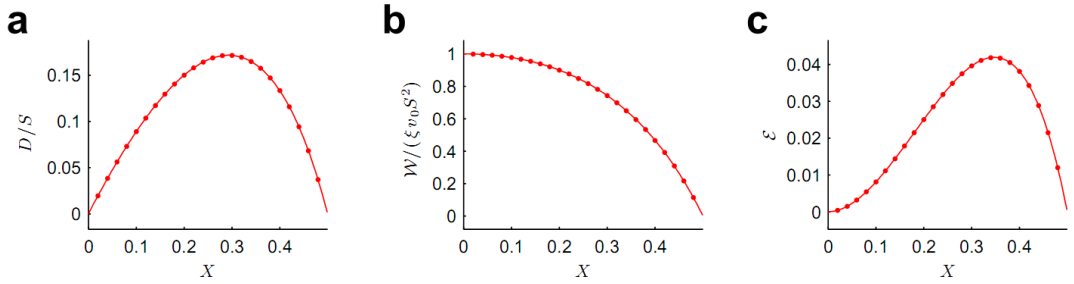

Figure 5: Comparison of the analytical to numerical results for the infinite square.

at $X = .2928$, $\tilde{U}_{v_0} = .1716$. The optimum for the normalized work from Eq. 22 occurs at $X = .3473$, $\tilde{\mathcal{W}}_{v_0} = .0419$

4.4 Cartesian Sine

The waveform for the cartesian sine is defined as follows (see Fig. 3):

$$y(x) = \frac{\lambda_x m}{2\pi} \sin\left(\frac{2\pi x}{\lambda_x}\right) \tag{23}$$

We start by defining the tangent as:

$$\hat{\mathbf{t}} = \begin{pmatrix} 1 \\ \\ y'(x) \end{pmatrix} / \sqrt{1 + y'(x)^2} \tag{24}$$

Note that the relationship for the wavelength along the x-axis and along the arc length is

$$\lambda = \int_0^{\lambda_x} \sqrt{1 + y'(x)^2} dx \ . \tag{25}$$

Since the filament is only moving in the x direction, the forces along the y-direction can be ignored. Accordingly, the local velocity of points on the filament are $U_x + v_0\hat{\mathbf{t}}$, and from

Eq. (4) the force is

$$dF_x = \xi \left(U_x \left(2 - \frac{1}{1 + y'(x)^2} \right) + \frac{v_0}{\sqrt{1 + y'(x)^2}} \right) ds \tag{26}$$

Setting $F_x = 0$ for the force balance and solving for U_x, the net velocity is obtained by integrating $U_x + v_0 \hat{\mathbf{t}}$ over one undulatory cycle

$$D_x = \mathrm{sgn}(v_0) \lambda \left(\frac{2\pi}{2\lambda - \int_0^{2\pi} \frac{dx}{\sqrt{1+y'(x)^2}}} - \frac{2\pi}{2\lambda} \right) \tag{27}$$

From here we take a Taylor expansion of the function around $m = 0$ and integrate it to arrive at the displacement:

$$\frac{D_x}{\lambda} = \frac{1}{2} m^2 - \frac{11}{16} m^4 + \frac{109}{128} m^6 \tag{28}$$

Substituting for D_x from Eq. 28 we calculate the power dissipated by one wavelength:

$$P = \xi \int_0^{\lambda} \left\{ U_x^2 \left(2 - t_x^4 \right) + 2 v_0 U_x t_x \left(2 - t_x \right) + v_0^2 \right\} ds \tag{29}$$

Taking another Taylor expansion about $m = 0$ and comparing to the power required to pull a straight filament to the power required for the actuated filament we get the efficiency:

$$\tilde{\mathcal{W}}_{v_0} = \frac{1}{4} m^2 - \frac{53}{128} m^4 + \frac{2289}{4096} m^6 \tag{30}$$

We can compare our result for the swimming speed with that of G. I. Taylor [7] who found the expansion:

$$U_{\text{Taylor}} = \frac{1}{2} b^2 - \frac{19}{32} b^4, \tag{31}$$

which varies in the fourth order term. This is puzzling as we would expect hydrodynamic effects which were neglected in resistive force theory to lead to an overestimate of the swimming speed. One possible resolution of this conundrum is that Taylor uses λ_x whereas our formulation uses the wavelength measured by arc length.

4.5 Curvature Sine

We start by defining the tangent in the following way:

$$\theta(s) = \alpha \cos(\frac{2\pi s}{\lambda}) \tag{32}$$

$$\hat{\mathbf{t}} = \begin{pmatrix} \cos(\theta(s)) \\ \\ \sin(\theta(s)) \end{pmatrix} \tag{33}$$

$$\tag{34}$$

The infinite nature of the filament again allows the y-components of the force to be ignored. The local velocity of points on the filament is $U_x\hat{\mathbf{x}} + v_0\hat{\mathbf{t}}$, and with Eq. (4) the force is

$$dF_x = \xi \left(2U_x \sin(\theta(s))^2 + U_x \cos(\theta(s))^2 + v_0 \cos(\theta(s))\right) ds \tag{35}$$

Setting $F_x = 0$ for the force balance gives $U_x = U_x = -v_0 \cos(\theta(s))/(\sin(\theta(s))^2 + 1)$. The net velocity is obtained by averaging $U_x + v_0\hat{\mathbf{t}}$ over one undulatory cycle

$$\mathbf{D} = \mathrm{sgn}(v_0) \int_0^\lambda \left(\hat{\mathbf{t}} - \frac{\cos(\phi(s))}{\sin(\theta(s))^2 + 1}\hat{\mathbf{x}}\right) ds \tag{36}$$

From here we take a Taylor expansion around $\alpha = 0$ of the function and integrate it to arrive at the displacement:

$$\frac{D_x}{\lambda} = \frac{1}{2}\alpha^2 - \frac{11}{16}\alpha^4 + \frac{421}{1152}\alpha^6 \tag{37}$$

Taking another Taylor expansion around $\alpha = 0$ and comparing to the power required to pull a straight filament to the power required for the actuated filament we get the efficiency:

$$\tilde{\mathcal{W}}_{v_0} = \frac{1}{4}\alpha^2 - \frac{41}{128}\alpha^4 + \frac{9529}{36864}\alpha^6 \tag{38}$$

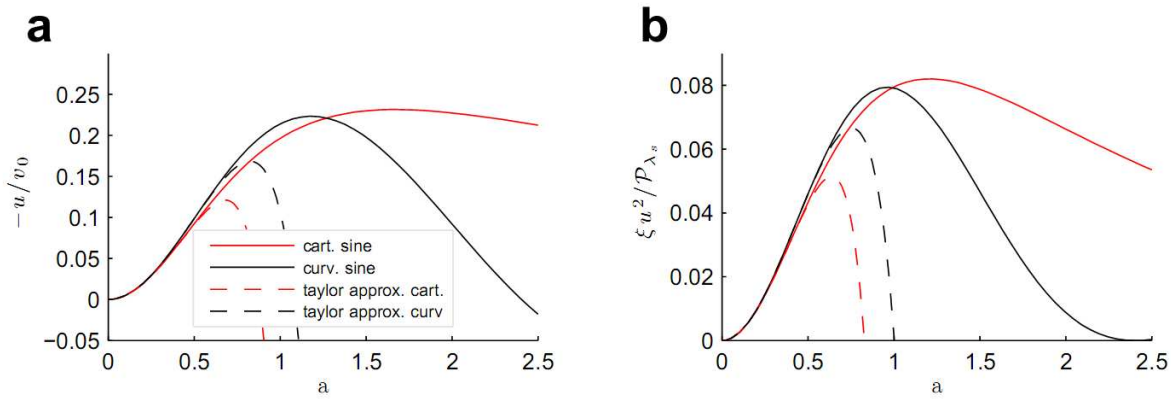

Figure 6: Comparison of the analytical to numerical results for the sinusoidal strategies for a) the speed b) the work efficiency

Fig. 6 shows several different methods for approximating the cartesian and curvature sines. The approximations are very close up until around $a = .5$. At this point the approximations diverge from the expected results.

When we compare the result we found for the swimming speed of the cartesian sine with the results that G. I. Taylor [7] found we see a slight difference. This difference is due to the simplifications that resistive force theory makes. The theory suggests that the difference due to neglected hydrodynamic effects would appear in the fourth order term.

$$U_{\text{Taylor}} = \frac{1}{2}b^2 - \frac{19}{32}b^4 \tag{39}$$

$$U_{\text{E}} = \frac{1}{2}m^2 - \frac{11}{16}m^4 + \frac{109}{128}m^6 \tag{40}$$

For the cartesian sine we get a maximum velocity and efficiency of:

$$\tilde{U}_{max} = .231 \tag{41}$$

$$\tilde{\mathcal{W}}_{max} = .082 \tag{42}$$

$$\tag{43}$$

And for the curvature sine we get:

$$\tilde{U}_{max} = .223 \tag{44}$$

$$\tilde{\mathcal{W}}_{max} = .07938 \tag{45}$$

Both of these values fall below the maximum efficiency of the sawtooth (0.238, 0.0858).

4.6 Summary

The results of this section are summarized in Table 1. The sawtooth is the most efficient of the infinite strategies. With the exception of the square wave, the other waveforms all have fairly similar efficiencies. Looking at the speed of the filaments we find the sawtooth is also the fastest swimmer, although again, with the exception of the square wave, all the swimming speeds are fairly close.

5 Symmetries and Pitching

One of the most readily observable differences between a finite length swimmer and an infinite length swimmer is that the finite length swimmer pitches, while the infinite swimmer does

Waveform	Parameter	$\tilde{U}_{v_0}$	Parameter	$\tilde{\mathcal{W}}_{v_0}$
cartesian Sine	m =1.048	.231	m =.888	.082
Curvature Sine	α =1.181	.223	α =.962	.079
Sawtooth	β =1.694	.238	β =1.398	.086
Square	X =.2928	.172	X =.347	.042

Table 1: Results for Infinite Filaments

not. The infinite swimmer has balanced torques along its length, and as we prove later the symmetries of the infinite case does not allow for pitching. To understand the pitching that occurs during a finite length filaments swimming cycle it helps to look at the symmetries of the problem.

The two major symmetries of the problem, point-wise and mirror, are shown in Fig. 7. The point-wise symmetry occurs about the filament's midpoint when $\mathbf{r}(s) = -\mathbf{r}(S-s)$. For mirror symmetry the reflection line is through the midpoint and transverse to the centerline, such that for every point on the filament (x, y) there is a reflected point at $(-x, y)$.

Throughout one swimming cycle, no matter what waveform is used, a swimmer goes through the point-wise and mirror symmetry states twice for a total of 4 points of symmetry. It can easily be seen in the point symmetry case that for every tangent along the wave, there will be an equal and opposite tangent elsewhere. This results in no pitching and purely horizontal movement as described in Fig. 8.

The following argument is illustrated in Fig. 8. When looking at the thrust torques for the mirror symmetry case we can see that unlike point symmetry this is a state of maximal

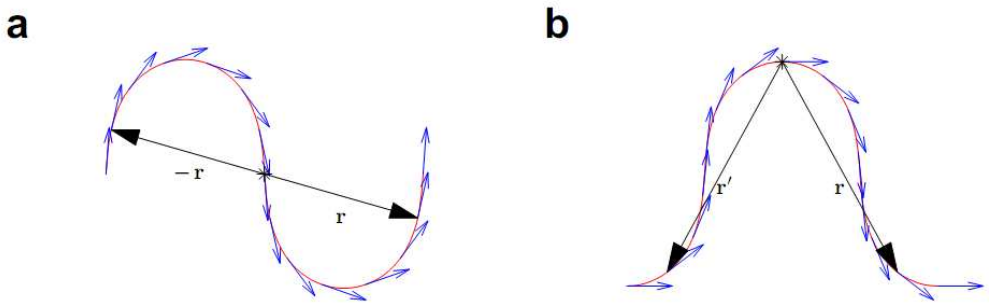

Figure 7: The point symmetry and mirror symmetry cases. Here $S = 1$ and $\alpha = 1.5$

pitching. However as we will now show, there is no pitching and again the motion is purely in the horizontal direction. As an example assume that there is a displacement with a vertical component. When we apply time symmetry we get a resultant displacement that is opposite the original displacement. If we apply mirror symmetry to the original displacement we get a reflected vector with a negative vertical component. The only way these two results are compatible is if there is no vertical displacement at this instant in time.

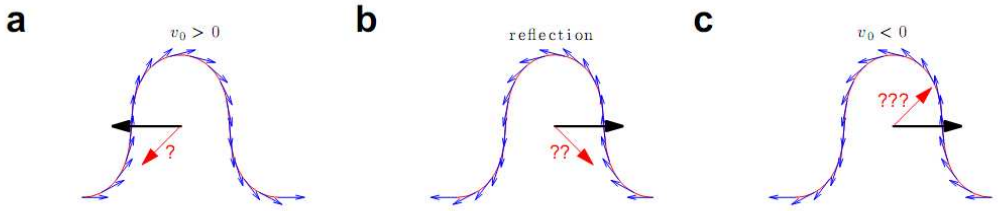

Figure 8: Mirror symmetry arguments for the displacement. The black arrow shows the actual displacement, the red arrow shows the contradictory vertical components. a) Positive wave speed, b) reflection about the vertical, c) negative wave speed

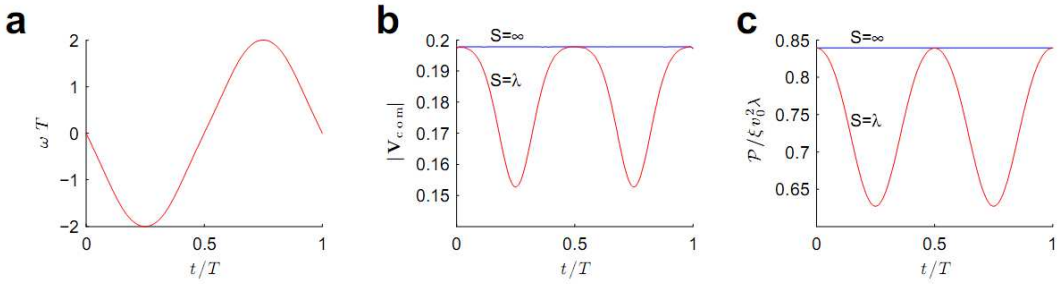

Figure 9: Dynamics of the curvature sine filament, with $\alpha = 1.5$, and $S = \lambda,\ \infty$. a) Pitching velocity of the finite-length filament. b) Speed of the center of mass. c) Power dissipated. The net displacements are $D/\lambda = 0.179,\ 0.198$ for the finite and infinite length filaments. No pitching occurs when $\omega T = 0, 1/2, 1$ which corresponds to the infinite case.

Having explored the symmetries the next important topic to cover is pitching. These arguments are qualitatively shown in video appendix b. Intuitively it is easy to see that pitching is undesirable. The more that a swimmer pitches the more energy it wastes. This

is shown more concretely in Fig. 9 where the finite length swimming speed oscillates along with its power dissipated. The infinite length however does not pitch and as a result is able to move quickly.

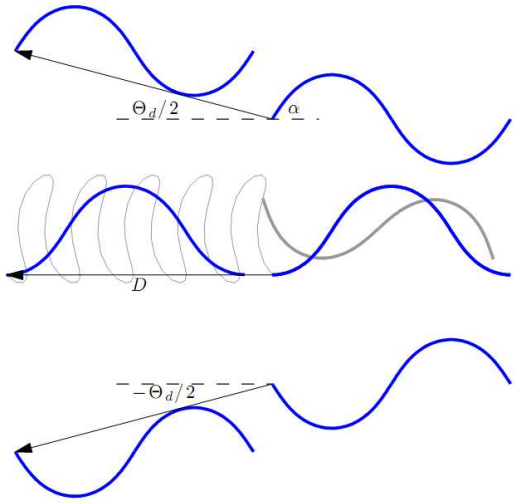

Figure 10: Cartoon of a filament length $S = \lambda$ performing five undulations employing the curvature sine strategy with amplitude $\alpha = 1$. The total distance traveled is $5D = 0.854\lambda_s$. The starting configurations differ by a phase angle of $\pi/2$, and the span of the drift angles is $\theta_d = 0.517$.

A direct result of pitching is drift. Drifting of filaments is illustrated in Fig. 10. This figure demonstrates that the net swimming direction is determined by the starting configuration. Only for a certain configuration will the filament move along its axis in a straight line.

6 Intermediate Length Swimmers

This section presents numerical solutions for all four finite length swimmers. The simulation was setup in Matlab using a quadrature rule to solve the force and torque integrals, and then the resultant differential equations were solved using `ode45`. This code can be seen in Appendix A.

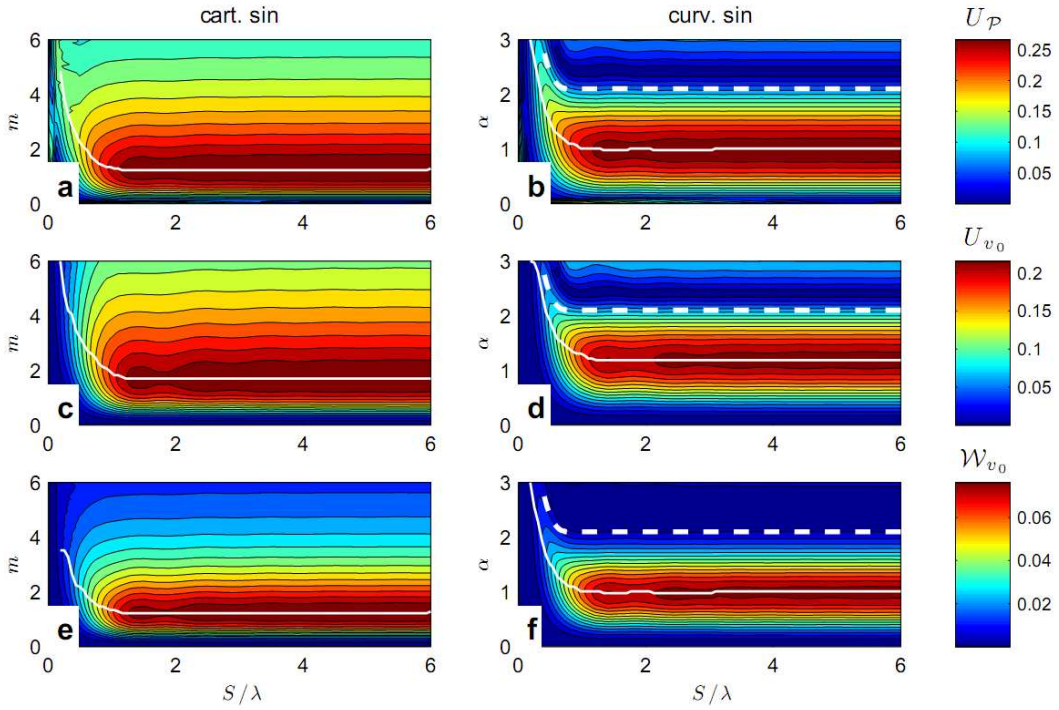

Figure 11: Parametric plots for the performance of the cartesian and curvature sine strategies: a-b) show the normalized velocity for constant power, c-d) show the normalized velocity for constant wave speed, and e-f) show the normalized work for constant wave speed. The white line shows dependence of the optimal value for m or α on S. The dashed white line indicates the region where the filament self-intersects.

Fig. 11 shows the parametric plots for all three performance criteria for both sinusoidal strategies. It is observed for both strategies that there are distinctly larger maximal areas around the half-integer wavelengths. This corresponds to the minimal pitching swimmers and optimal strategies. The white lane traces the optimal parameter for a given filament length. Both plots show that around the maximal strategy the filament is not effected by small perturbations, but that the performance plateau falls off quickly.

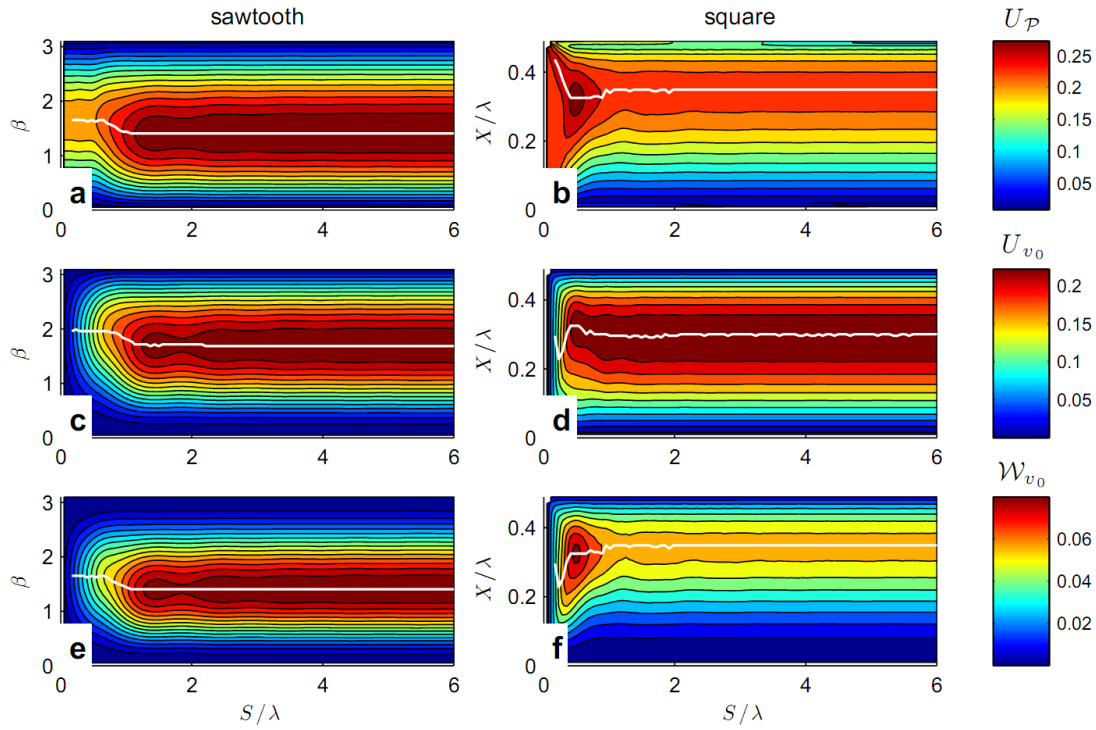

Figure 12: Parametric plots for the performance of the sawtooth and square strategies: a-b) show the normalized velocity for constant power, c-d) show the normalized velocity for constant wave speed, and e-f) show the normalized work for constant wave speed. The white line shows dependence of the optimal value for X or β on S

Fig. 12 shows the parametric plots for the sawtooth and square strategies. The sawtooth strategy behaves similarly to changes in parameters to the sinusoidal strategies, but manages to achieve a higher maximal value. The square wave behaves in a completely different way. There is a small island of optimal performance at small filament lengths that is due to the fact that the square strategy utilizes pitching in its movement.

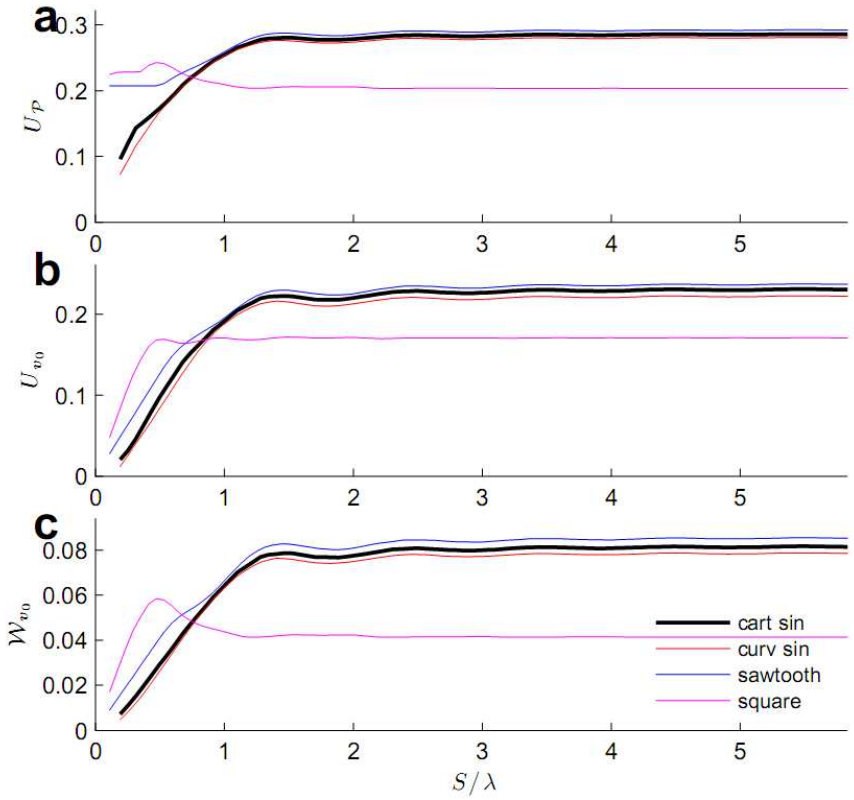

Figure 13: Dependence of the optimal swimming performance for a) speed at constant power, b) speed at constant wave speed, and c) work at constant wave speed on filament length.

One conclusion that can be drawn from the plots is illustrated in Fig. 13. The parametric study was limited to filaments of length $S/\lambda = 6$, however if the study was expanded to longer

and longer filaments there would continue to be slightly higher efficiencies. However even at $S/\lambda = 6$ the answer approaches the value for an infinite solution to within a a half percent.

Table 2: Optima of swimming performance using three criteria.

	param.	S	$U_{\mathcal{P}}$	param.	S	U_{v_0}	param.	S	$\mathcal{W}_{v_0}$
sawtooth	1.40	5.48λ	0.293	1.69	5.49λ	0.238	1.40	5.49λ	0.086
square	0.32	0.49λ	0.244	0.29	1.53λ	0.172	0.33	0.50λ	0.059
curv. sin	0.96	5.5λ	0.281	1.2	5.5λ	0.223	0.96	5.5λ	0.0792
cart. sin	1.2	5.5λ	0.286	1.7	5.5λ	0.231	1.2	5.5λ	0.0818

Table 6 shows the optimal values for all four swimming strategies. Video appendix C. shows the swimming speed results qualitatively. Again the square wave stands out from the other strategies. We see that all the other strategies are fairly close for the performance criteria, but the square lags behind. The sawtooth proves again to be the optimal strategy for all parameters.

7 Conclusions

We have researched four possible swimming strategies. For both finite and infinite swimmers we find the sawtooth to be the fastest and most efficient with both sinusoidal strategies close. The square strategy is found to fall well below the rest. We also investigated into pitching and the effects it has on swimming. We were able to conclude that although the longer a filament is the less pitching it has, there is also a local minimum around half integer wavelengths. These half integer wavelengths form a group of optimal swimming strategies.

This research has many applications, such as cell motility. Spermatozoa are a prime example of a low Reynolds swimmer that might have traits in common with our swimming strategy. There are also direct applications to swimming robots. If a robots shape resembles a long filament and swims at low Reynolds number then our study can help identify optimal swimming strategies.

There are many opportunities for future research. One of the most basic expansions would be to consider swimmers in three dimensions. This would involve reformulating the problem in the director basis as introduced by [16] This brings up a much larger parameter space which allows for new swimming strategies. It could be very interesting to consider waveforms without the symmetries imposed by our study. This exploration of waveforms could be definitively answered by setting up and solving the full variational problem. One final further opportunity would be to expand resistive force theory to other materials which rely on a drag anisotropy. Finally resistive force theory can be adapted for other fluid like materials such as granular matter [17]

References

[1] J. Lighthill. *Mathematical biofluiddynamics*. Regional conference series in applied mathematics. Society for Industrial and Applied Mathematics, 1975.

[2] S Humphries, J P Evans, and L W Simmons. Sperm competition: linking form to function. *BMC Evol Biol*, 8:319–319, 2008.

[3] E. Lauga and T. Powers. The hydrodynamics of swimming microorganisms. *Reports on Progress in Physics*, 72(9):096601, 2009.

[4] R Rikmenspoel. Movements and active moments of bull sperm flagella as a function of temperature and viscosity. *J Exp Biol*, 108:205–230, Jan 1984.

[5] E. A. Gillies, R. M. Cannon, R. B. Green, and A. Pacey. Hydrodynamic propulsion of human sperm. *Journal of Fluid Mechanics*, 625(-1):445–474, 2009.

[6] D. J. Smith, E. A. Gaffney, H. Gadêlha, N. Kapur, and J. C. Kirkman-Brown. Bend propagation in the flagella of migrating human sperm, and its modulation by viscosity. *Cell Motility and the Cytoskeleton*, 66(4):220–236, 2009.

[7] G. I. Taylor. Analysis of the swimming of microscopic organisms. *Proceedings of the Royal Society of London. Series A. Mathematical and Physical Sciences*, 209(1099):447–461, November 1951.

[8] J. Gray and G. J. Hancock. The propulsion of Sea-Urchin spermatozoa. *J Exp Biol*, 32(4):802–814, December 1955.

[9] J. B. Keller and S. I. Rubinow. Slender-body theory for slow viscous flow. *Journal of Fluid Mechanics Digital Archive*, 75(04):705–714, 1976.

[10] J. Lighthill. Flagellar hydrodynamics: The john von neumann lecture, 1975. *SIAM Review*, 18(2):161–230, 1976.

[11] E. Purcell. Life at low reynolds number. *American Journal of Physics*, 45(1):3–11, 1977.

[12] L. E. Becker, S. A. Koehler, and H. A. Stone. On self-propulsion of micro-machines at low reynolds number: Purcell's three-link swimmer. *Journal of Fluid Mechanics*, 490:15–35, 2003.

[13] Daniel Tam and A. E. Hosoi. Optimal stroke patterns for purcell's Three-Link swimmer. *Physical Review Letters*, 98(6):068105, February 2007.

[14] O. Pironneau and D. F. Katz. Optimal swimming of flagellated micro-organisms. *Journal of Fluid Mechanics*, 66(02):391–415, 1974.

[15] S. E. Spagnolie and E. Lauga. The optimal elastic flagellum. *Physics of Fluids*, 22(3):031901, March 2010.

[16] Goriely A. and Tabor M. Nonlinear dynamics of filaments i. dynamical instabilities. *Physica D: Nonlinear Phenomena*, 105(1-3):20 – 44, 1997.

[17] Goldman D. and Hu D. Wiggling through the world. *American Scientist*, 98(4):314, 2010.

A Video Appendix

Appendix VA. Demonstration of a Swimming Filament

Appendix VB. Demonstration of Pitching

Appendix VC. Optimal Finite Length Swimmers

B Small Amplitude Swimmers

This section provides a brief summary of solutions found for small amplitude undulations.

B.1 Sawtooth

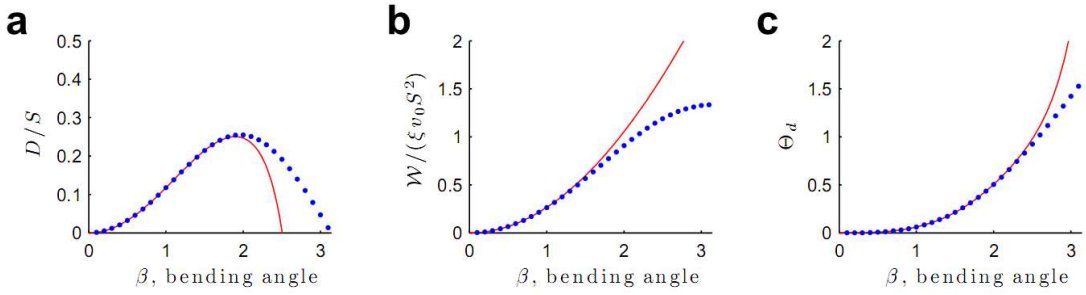

Figure 14: Comparison of Taylor series approximations with numerical results for the sawtooth

$$\frac{D}{S} = \frac{25488131797}{363424501440000}\alpha^{10} + \frac{48166973}{188972784000}\alpha^{8} - \frac{718799}{367567200}\alpha^{6} - \frac{16}{1155}\alpha^{4} + \frac{2}{15}\alpha^{2} \quad (46)$$

$$\mathcal{W} = \frac{336}{1260}\alpha^{2} - \frac{1}{1260}\alpha^{4} \quad (47)$$

$$\theta_d = -\frac{17}{25200}\alpha^{7} + \frac{13}{3360}\alpha^{5} + \frac{7}{120}\alpha^{3} \quad (48)$$

These values were calculated using a Taylor approximation before evaluating the force integral and then again before solving the system of differential equations. We find values that match with the numerical values found in the previous section.

B.2 Square

$$\boldsymbol{\Delta}\left(t=\frac{1}{4}\right)=\begin{bmatrix}0.2091\\0.1688\end{bmatrix} \tag{49}$$

$$\theta\left(t=\frac{1}{4}\right)=0.4928 \tag{50}$$

$$\boldsymbol{\Delta}\left(t=\frac{1}{2}\right)=\left(1+\mathcal{R}\left(\theta\left(t=\frac{1}{4}\right)\right)\right)\boldsymbol{\Delta}\left(t=\frac{1}{4}\right)=\begin{bmatrix}0.3134\\0.4164\end{bmatrix} \tag{51}$$

$$\theta\left(t=\frac{1}{2}\right)=2\theta\left(t=\frac{1}{4}\right) \tag{52}$$

$$\boldsymbol{\Delta}\left(t=1\right)=\left(1+\begin{bmatrix}-1&0\\0&1\end{bmatrix}\mathcal{R}\left(-\theta\left(t=\frac{1}{2}\right)\right)\right)\boldsymbol{\Delta}\left(t=\frac{1}{4}\right)=\begin{bmatrix}-0.2068\\0.3851\end{bmatrix} \tag{53}$$

$$\theta\left(t=1\right)=0 \tag{54}$$

$$\theta_d = 0.4928 \tag{55}$$

B.3 Curvature Sine

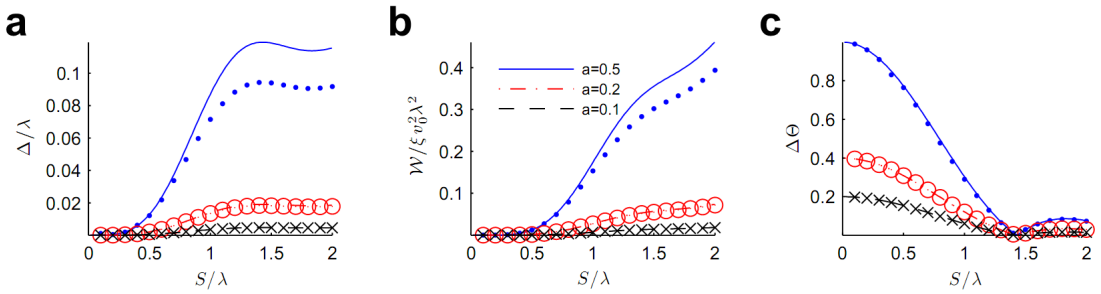

Figure 15: Comparison of Taylor series approximations with numerical results for the curvature sine

The displacement for a finite-length undulating curvature sin waveform is $\kappa = \frac{a}{\lambda}\sin(2\pi s/\lambda)$

$$\frac{\Delta}{\lambda} = -\left(\frac{a^2}{2}\right)\left[1 + \frac{3\lambda^4}{\pi^4 S^4}\left(\cos(\pi S/\lambda)^2 - 1\right) - \frac{\lambda^2}{\pi^2 S^2}\left(2\cos(\pi S/\lambda)^2 + 1\right) + \frac{12\lambda^3}{\pi^3 S^3}\sin(2\pi S/\lambda)\right] \quad (56)$$

The work required for one undulation is

$$\frac{\mathcal{W}}{\xi v_0^2 \lambda^2} = a\left[\frac{S}{\lambda} + \frac{3\lambda^3}{\pi^4 S^3}\left(\cos(\pi S/\lambda)^2 - 1\right) - \frac{\lambda}{\pi^2 S}\left(2\cos(\pi S/\lambda)^2 + 1\right) + \frac{3\lambda^2}{\pi^3 S^2}\sin(2\pi S/\lambda)\right] \quad (57)$$

B.4 Cartesian Sine

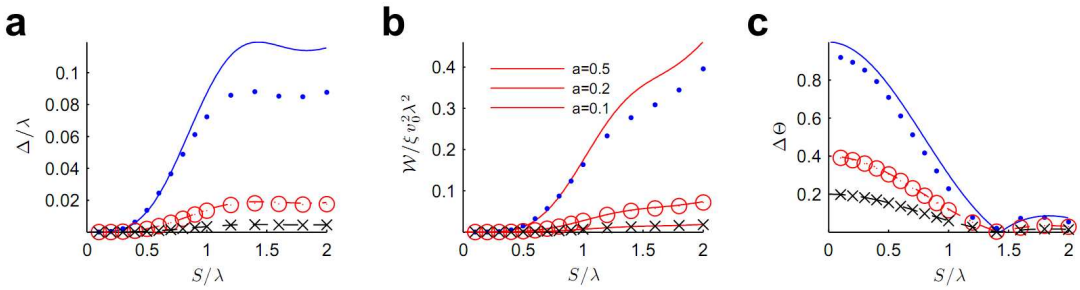

Figure 16: Comparison of Taylor series approximations with numerical results for the cartesian sine

The displacement for a finite-length undulating curvature sin waveform is $y = \frac{a\lambda}{2\pi}\sin(2\pi x/\lambda)$

$$\frac{\Delta}{\lambda} = \left(\frac{a^2}{2}\right)\left[1 - \frac{3\lambda^4}{2\pi^4 X^4}\left(1-\cos(2\pi X/\lambda)\right) - \frac{\lambda^2}{\pi^2 X^2}\left(2+\cos(2\pi X/\lambda)^2\right) + \frac{3\lambda^3}{\pi^3 X^3}\sin(2\pi X/\lambda)\right] \quad (58)$$

The work required for one undulation is

$$\frac{\mathcal{W}}{\xi v_0^2\lambda^2} = a^2\left[\frac{X}{\lambda} - \frac{\lambda}{\pi^2 X}\left(1+2\cos(\pi X/\lambda)^2\right) + \frac{3}{\pi^3 X^3}\sin(2\pi X/\lambda) - \frac{3}{\pi^4 X^3}\left(1-\cos(\pi X/\lambda)^2\right)\right] \quad (59)$$

C Matlab

See the attached Matlab folder.